JOURNAL OF GEOPHYSICAL RESEARCH, VOL. 94, NO. D9, PAGES 11,223–11,231, AUGUST 30, 1989

Observational Results Using the Microwave Temperature Profiler During the Airborne Antarctic Ozone Experiment

BRUCE L. GARY

Jet Propulsion Laboratory, California Institute of Technology, Pasadena

The Microwave Temperature Profiler (MTP) measures profiles of air temperature versus altitude. The altitude coverage is about 5 km at a flight altitude of 20 km (66,000 feet), and the profiles are obtained every 14 s. The MTP instrument is installed on NASA's ER-2 aircraft, which flew 13 missions over Antarctica during the Airborne Antarctic Ozone Experiment. Altitude temperature profiles were used to derive potential temperature cross sections. These cross sections have been useful in detecting atmospheric waves. Many wave encounters have been identified as "mountain waves." The mountain waves are found to extend from the lowest altitudes measured to the highest (about 24 km). The southern part of the Palmer Peninsula was found to be associated with mountain waves more than half the time. Altitude temperature profiles were also used to measure the lapse rate along the flight track. Lapse rate versus latitude plots do not show significant changes at the ozone hole boundary.

1. INTRODUCTION

The Microwave Temperature Profiler (MTP) is the only airborne instrument of its kind. It was installed on NASA's ER-2 aircraft in 1985 for the Stratospheric Tropospheric Exchange Experiment (STEP). Its function for STEP was to measure the lapse rate along the flight track, so that potential vorticity could be calculated. Potential vorticity was to be used to identify air in the stratosphere that had recently originated in the troposphere.

A predecessor to the MTP was installed in NASA's C-141 Kuiper Airborne Observatory. It was used to evaluate the merits of providing flight level change advisories to pilots for avoiding encounters with clear-air turbulence (CAT). Data from this flight series demonstrated the association of CAT with such temperature field features as the tropopause and inversion layers.

The MTP instrument was selected for inclusion on the AAOE mission to assist in locating the polar vortex boundary, using potential vorticity as a tracer. Potential vorticity requires knowledge of the horizontal gradient of wind, provided by the Meteorology Measurement System (MMS), and the vertical gradient of air temperature, provided by the MTP. It was anticipated that one or both of these meteorological quantities would undergo a change when passing through the polar vortex boundary.

2. REMOTE SENSING PRINCIPLES

The MTP instrument is a passive microwave radiometer, operating at the frequencies of 57.3 and 58.8 GHz. It weighs 55 pounds (~25 kg) and is mounted on the outer side of the left wing pod on the ER-2. A more complete description of the physical and electronic attributes of MTP is given by [*Denning et al.*, 1989].

MTP measures "brightness temperature" at a selection of 10 elevation angles every 14.0 s. Oxygen molecules are the principal source of thermal emission at these frequencies. A measurement of the temperature of oxygen molecules is equivalent to a measurement of air temperature.

Brightness temperature is actually a weighted integral of air temperature along the instrument's viewing direction. The weighting function has a shape that is quasi-exponential, decreasing with range to $1/e$ at a distance of about 1.5 km at 58.8 GHz and 3 km at 57.3 GHz. The absorption coefficient of oxygen depends on air temperature as well as density, and these second-order effects must be taken into account when converting observable quantities to profiles of air temperature. The oxygen absorption model of *Rosenkranz* [1975] has been used.

As an approximation, the MTP can be thought of as measuring air temperature at a location specified by the $1/e$ range of each channel. Since measurements are made with both channels at 10 elevation angles, there are 20 air temperature locations, which are specified by the equation

$$A_i = A_0 + L*\text{sine}\ (E)$$

where A_i is the altitude of the air whose temperature is being measured, A_0 is the altitude of the aircraft, L is the "applicable range" of the channel in question (the $1/e$ range), and E is the elevation angle of the observation. Because some of the A_i of one channel are approximately the same as for the other channel, there are, in effect, only 15 "applicable altitudes."

The altitude coverage of the MTP instrument is greater at the higher altitudes. This is due to the fact that applicable range is inversely proportional to air density.

At the highest flight levels the atmosphere's opacity is insufficient to absorb all microwave radiation along the slant paths corresponding to the high-elevation angles (i.e., +60°). This leads to a "transparency correction," which must be applied before brightness temperatures can be converted to air temperatures. This correction term grows rapidly with altitude at the high elevation angles, and it can be as great as 30 K.

A more complete description of remote sensing concepts that apply to the MTP instrument is given in the appendix.

Paper number 89JD00857.
0148-0227/89/89JD-00857$05.00

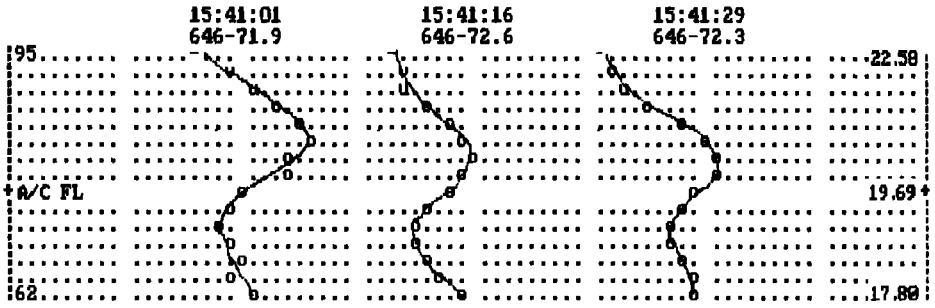

Fig. 1. A sequence of three altitude temperature profiles. Each column represents 0.25 K, and each row represents approximately 1100 feet. (0.34 km). The ER-2 flight level is 64,600 feet (or 19.69 km), pressure altitude. Note the inversion layer structure and its slight changes.

3. OBSERVATIONAL PRODUCTS

Altitude Temperature Profiles

The MTP's basic observational product is air temperature at 15 altitudes every 14 s, as illustrated in Figure 1. The profiles in Figure 1 were taken during level flight at 64,600 feet or about 19.6 km (pressure altitude). The temperature scale is 0.25 K per column. The altitude scale extends from 6200 feet below to 9500 feet (~2–3 km) above flight level. Pressure altitudes (in kilometers) are shown on the right. Below the time blocks are flight level (in units of 100 feet) and outside air temperature (in degrees celsius). Figure 1 shows that the aircraft is flying within an inversion layer that is 5000 feet (1.5 km) thick and is about 1.4 K warmer at the top than at the bottom. Slow changes in inversion layer properties are evident.

Lapse Rate

From the altitude temperature profiles it is possible to calculate lapse rate, defined here to be dT/dz, by comparing temperatures at altitudes above and below flight level. It has been possible to evaluate the accuracy of MTP-derived lapse rates during slow ascents and descents by making use of in situ measurements of air temperature made by the Meteorology Measurement System (MMS) [*Chan et al.*, 1989. S. G. Scott et al., manuscript in preparation, 1989]. The MMS air temperature data were plotted versus altitude and "air truth" lapse rates were derived (which assumes that horizontal gradients were small). In each case when this has been done, the MTP lapse rates agree with the MMS-derived values. For example, on the flight of September 22, 1987, there is a 2-min period when MTP measured a lapse rate of -8.9 ± 0.2 K km^{-1}. This occurred during the descent at the southernmost part of the flight. MMS air temperature versus altitude data were used to predict that the MTP should have measured 8.8 ± 0.3 K. In spite of this excellent agreement (difference = 0.1 ± 0.4 K km^{-1}, or $1.1 \pm 3.3\%$), the MTP lapse rates are estimated to have an accuracy of about 10% of the measured value.

Figure 2 is a sample trace of lapse rate versus latitude for the flight of August 17, 1987. This lapse rate is for a layer that is 0.7-km thick, centered on the aircraft's flight level (which was relatively constant during this flight portion).

The fluctuations in this trace are actual lapse rate variations. The abrupt change at latitude 64.2°S, from +1 to −3 K km^{-1}, is somewhat unusual. Inspection of the temperature field at higher and lower altitudes than those used to produce this plot show that a wide range of altitudes underwent a change of air temperature at this latitude (mostly at the higher altitudes). The altitude difference between Θ surfaces (described later) that are 40 K apart showed a 27% change at this same location (from 2.2 to 2.8 km). This event illustrates

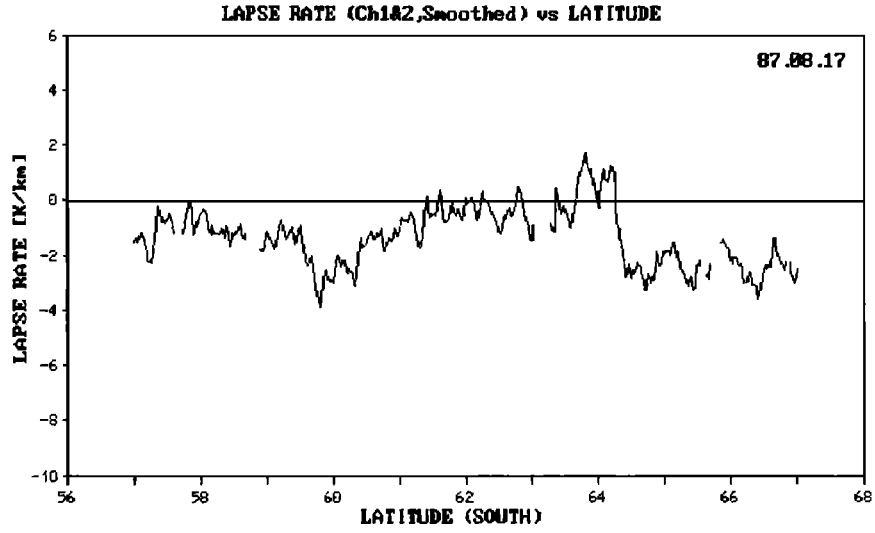

Fig. 2. Lapse rate versus latitude, for a layer that is 0.7-km thick, centered on the ER-2 flight level (62,000 feet).

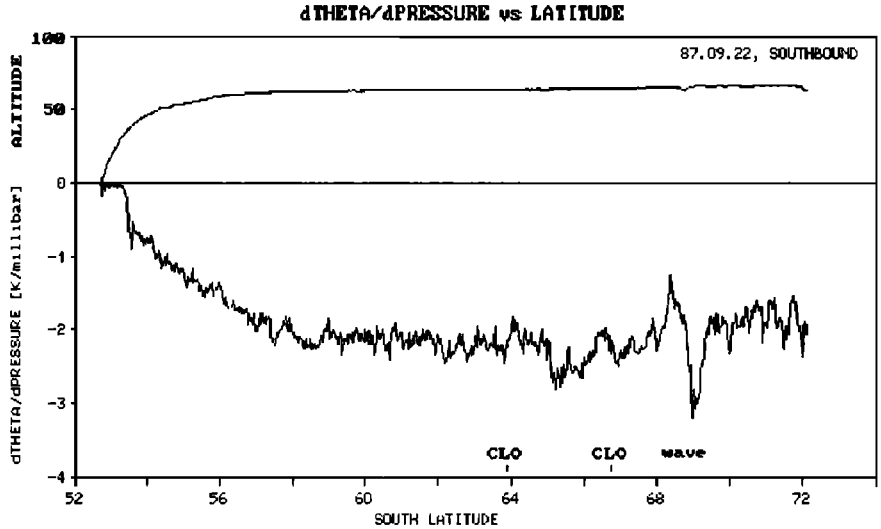

Fig. 3. Sample plot of $d\Theta/dP$ (potential temperature pressure gradient) versus latitude (lower plot). There is no marked change while penetrating into the region of high ClO/low ozone (southward of about 67°S). The upper plot is ER-2 flight altitude.

how MTP data can be used to characterize lapse rate aspects of the temperature field on layer scales of from 0.7 to about 3 km.

Potential Temperature Pressure Gradient

Profiles of air temperature can be converted to profiles of potential temperature by using standard equations. Potential temperature, Θ, is defined as $\Theta = T*(1000/P)^{0.286}$, where T is air temperature (in Kelvins), and P is air pressure (in mbar). Potential vorticity is primarily influenced by the product of horizontal gradient of wind and the pressure gradient of potential temperature, $d\Theta/dP$. The $d\Theta/dP$ term can be calculated from profiles of air temperature versus altitude by calculating Θ and P for each of the measured altitudes and taking a derivative at flight level. Figure 3 is a sample of this data.

The lower trace in Figure 3 is $d\Theta/dP$ for the southbound portion of the flight of September 22, 1987. The upper trace is ER-2 pressure altitude (in kilofeet). The notations "CLO" indicate the onset of chlorine monoxide increase (a second abrupt rise is indicated). A mountain wave (described later) was encountered at a latitude region 68.4° to 69.0°S.

Potential Temperature Cross Sections

Each altitude temperature profile can be converted to a profile of potential temperature, as described in the previous section. Interpolations can be made within these profiles to determine altitudes of specified potential temperature surfaces. A time series of such potential temperature surface altitudes can be used to create "potential temperature cross sections."

Figure 4 is a sample potential temperature cross section (Θ-CS). In Figure 4 the pressure altitudes for selected potential temperatures are plotted with coded symbols. The 400 K altitudes are plotted with large squares. Hand-fitted lines are shown for potential temperature surfaces at 10 K intervals. The trace at about 19 km (or 425 K) is the ER-2 flight level. Pressure altitude (in kilometers) is shown on the left. Latitude (ϕ) crossing times are indicated at the bottom. Universal time is given below the tick marks.

The Θ-CS graphs can be used to detect "waves" in the atmosphere. Since potential temperature is a conserved property on short time scales (when an air parcel does not gain or lose heat due to condensation or solar heating), surfaces of iso-Θ can be thought of as streamlines. When air parcels are forced to undergo altitude excursions, the Θ surfaces mark the paths of these parcel motions.

Potential temperature cross sections show waves of some amplitude and period almost all the time. The small undulations in the altitudes of the Θ surfaces of Figure 4 are typical. Generally, wave amplitudes are less than 200 m, peak-to-peak, and their wavelengths are longer than 100 km.

4. MOUNTAIN WAVE ENCOUNTERS

Identifying Characteristics

On 12 occasions, waves were encountered that differed in three ways from the typical wave: they had higher amplitudes (200–1200 m), much shorter wavelengths (typically 20 km), and they existed at all altitudes sampled (18–23 km, typically).

Figure 5 is a Θ-CS for the largest wave encounter. Note the flight level excursions, at 1615 to 1620 UT, caused by downdrafts and updrafts. The Θ surfaces exhibit altitude excursions that range from about 500 m at the low altitudes to 1200 m at the high altitudes. The location of the minima and maxima appear to be more spread out at the higher altitudes.

Amplitude Growth With Altitude

Mountain wave theory predicts that wave amplitude should increase with altitude as the inverse square-root of density [*Holton*, 1979]. The left-hand panel of Figure 6 is a plot of peak-to-peak amplitude versus pressure altitude for the 12 mountain wave events identified in this study. The right-hand panel is a replot of this data, with wave amplitude normalized in a way that places each event's average amplitude close to the fitted line.

On all occasions the winds increased with altitude from 6 to 24 km (pressure altitude), according to the United Kingdom Meteorology Office European Centre for Medium-

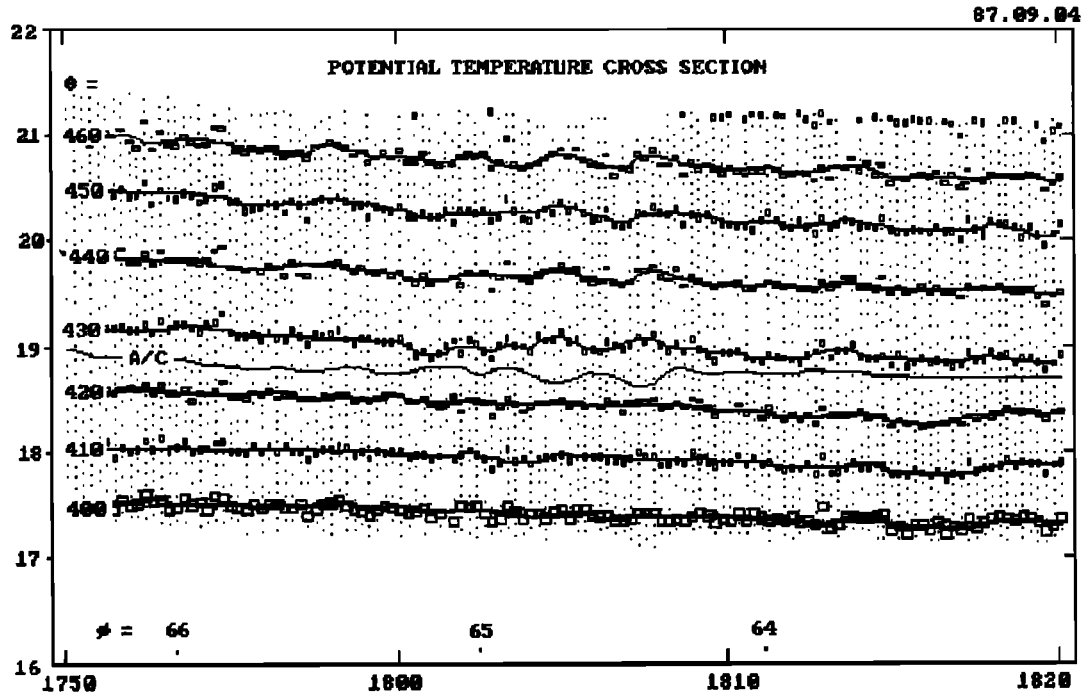

Fig. 4. Typical potential temperature cross section. The altitude of potential temperature surfaces is plotted with coded symbols and hand trace-fitted. The ER-2 flight altitude is indicated by the line labeled "A/C." Pressure altitude is shown on the left. UT times are shown at the bottom. Latitude crossing times are indicated below.

Range Weather Forecast (ECMWF) analysis [*McKenna et al*, 1989]. Average values are: 24 km (100 knots); 18 km (80 kt knots); 12 km (60 knots); 6 km (50 knots) (and extrapolated, 2 km (45 knots kt)). Wind direction varied little from 6 to 24 km, with averages of 292° and 279; respectively.

The fitted line in the right-hand panel of Figure 6 has the predicted shape of $1/\sqrt{P}$ (pressure can be used in place of air density, since temperature is approximately constant throughout this part of the stratosphere). Most of the observations are compatible with the predicted shape. This strengthens the case for identifying these wave events as "mountain" waves.

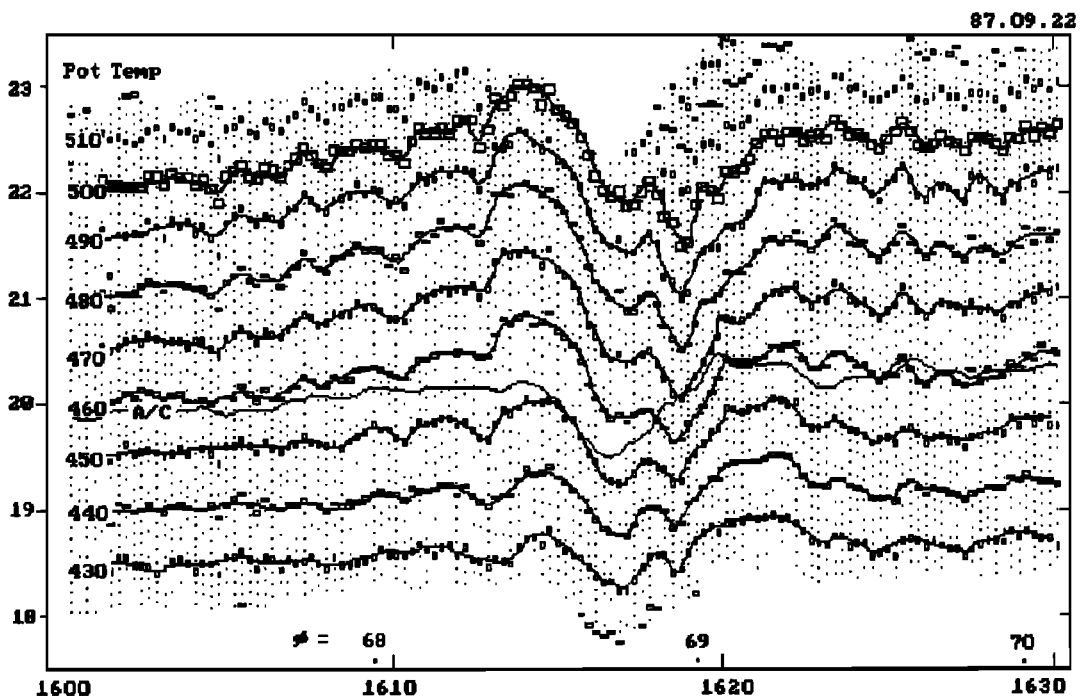

Fig. 5. Potential temperature cross section for a mountain wave encounter. The shape of the potential temperature surfaces are distorted differently at different altitudes.

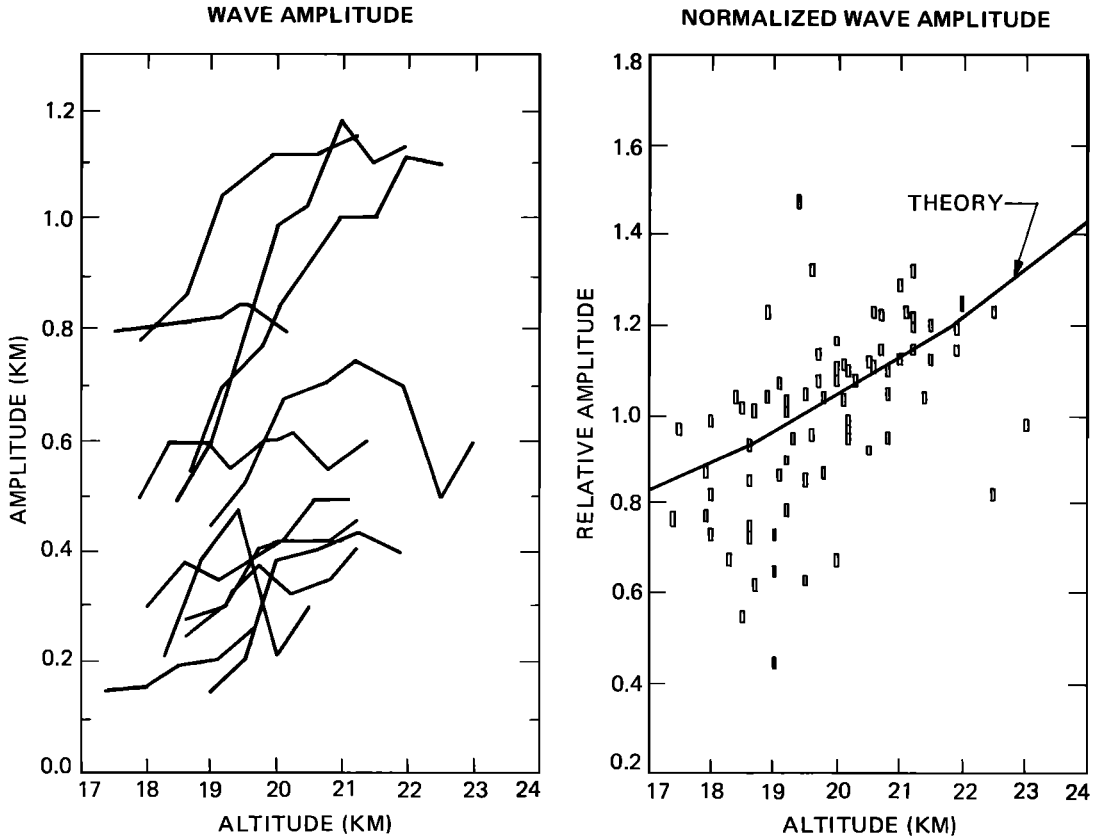

Fig. 6. (Left) Peak-to-peak amplitude of mountain waves versus pressure altitude. (Right) Amplitudes are normalized to permit comparisons of the variation of relative amplitude with altitude. Mountain waves are expected to exhibit a variation shown by the "theory" line.

Location of Encounters

An analysis of the location of the aircraft when these high-amplitude, short-period waves were encountered shows that they always occurred over the Palmer Peninsula. An analysis was made of the likelihood of encountering these waves for each of the latitude/longitude cells where at least three over-flights occurred. The left-hand panel of Figure 7 shows the average peak-to-peak wave amplitude on a map that includes all flight tracks. The right-hand panel of Figure 7 is the occurrence probability of the "subjectively" identified mountain wave encounters. Both methods for identifying mountain waves agreed in identifying the Palmer Peninsula as preferred locations for encounters. The waves were encountered at the south end of Palmer Peninsula 64% of the time. The northern half of the peninsula had an encounter probability of 30%. No encounters occurred over the ocean (beyond 100 km of land). Flights were not made near the eastern edge of the peninsula because the pilots noted wave clouds in those regions.

On three consecutive flights, September 20, 21, and 22, 1987, a short-period wave group was encountered at approximately the same location on both the outbound and inbound legs of the flight (that is, six encounters). Presumably this was the "same" wave that persisted for at least 3 days. It may have lasted longer, since the September was the last flight over the Palmer Peninsula.

There is a strong correlation of the high-amplitude/short-period/altitude extensive waves with the presence of underlying mountains. The frequent citing of lee wave clouds over the eastern edge of the Palmer Peninsula implies that the occurrence of mountain waves there was at least as frequent as over the western edge, where the flights occurred. This suggests that the entire Palmer Peninsula was producing mountain waves at least 30–64% of the time during the period of ER-2 observations.

Implications of Mountain Waves for Ozone Hole

Mountain waves that propagate into the polar vortex may have implications for the formation of the ozone hole. Upward excursions of air parcels lead to a brief cooling. This can begin the process of cloud formation. It is important to determine how much additional formation of polar stratospheric cloud (PSC) material is possible by the passage of air parcels through a mountain wave pattern that endures for long periods. Other mountain wave effects have been suggested, such as a speeding up of the vortex and a consequent cooling of large air volumes, which, in turn, might add to PSC production (D. Cariolle, personal communication, 1989).

5. Penetrations of the Polar Vortex and Ozone Hole

It remains to be demonstrated that the polar vortex and the "ozone hole" have the same boundaries. The polar vortex is generally thought of as the air mass whose parcel trajectories remain confined to high latitudes, whereas the ozone hole is the air mass that is deficient in ozone.

Since chlorine monoxide (ClO) is so well correlated with low ozone after the hole develops [*Anderson*, this issue], it is

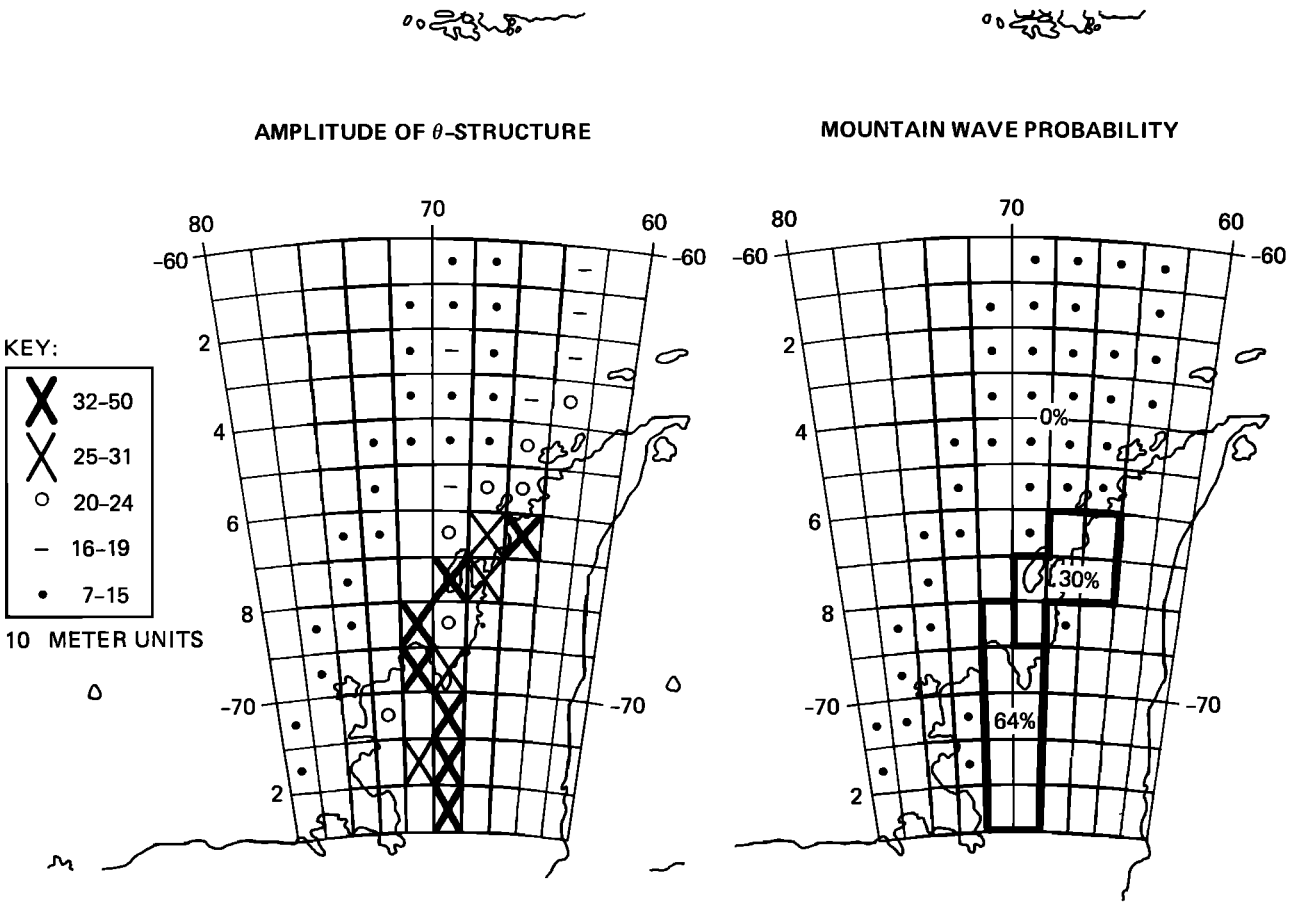

Fig. 7. Location of encounters with "mountain waves." (Left) The average wave amplitude (all categories of waves) versus geographical location. (Right) The encounter occurrence probability of "subjectively" identified mountain waves. Both panels indicate an association of wave activity with the Palmer Peninsula.

natural to refer to the high-ClO region prior to ozone loss as the ozone hole as well. A more accurate term for this high-ClO region is the "chemically perturbed region" (or chemical containment vessel, etc). In what follows, I shall use the term "ozone hole" to have this broader meaning, and ClO will be used to locate the ozone hole boundary.

Ideally, the polar vortex boundary would be determined by performing an extensive analysis of parcel trajectories backward in time in order to locate the region where trajectories have been confined to polar latitudes. Potential vorticity is generally recognized as providing an alternative and more convenient means for locating the polar vortex boundary. The ER-2 Meteorology Measurement System, measures wind vector versus time [*Chan et al.*, this issue; S. G. Scott et al., manuscript in preparation, 1989]. Combining this wind information with MTP measurements of lapse rate makes calculation of potential vorticity possible.

These calculations have been performed and are reported by *Hartmann et al.*, [this issue]. This work shows that on several flights potential vorticity can be used to locate the polar vortex boundary. Changes of potential vorticity can be produced by changes either in horizontal wind shear or in potential temperature lapse rate. The remainder of this section is confined to an exploration of correlations between MTP-measured lapse rate with penetrations of the polar vortex and ozone hole.

Figure 3 is a plot of potential temperature lapse rate versus latitude for a flight that penetrated the ozone hole (as defined by the presence of ClO). There is no apparent correlation of lapse rate with ClO. Plots for other penetrations show a similar lack of correlation. From this I conclude that lapse rate changes do not correlate with penetrations of the chemically perturbed ozone hole region.

Hartmann et al. [this issue] had to use a broad latitude smoothing to obtain useful plots of potential vorticity versus latitude. The polar vortex boundaries are therefore less well defined than the ozone hole boundary. It is necessary to impose a comparable smoothing on the lapse rate data. When this is done and comparisons are made, it is found that lapse rate does not undergo a marked change at the vortex boundary. I conclude that lapse rate does not change during penetrations of the vortex boundary at the altitudes flown during the Airborne Antarctic Ozone Experiment (AAOE).

6. Altitude Excursions and Tracer Correlations

The ER-2 had 15 experiment payloads, used to measure more than 12 atmospheric constituents, aerosols, and other properties. A large effort has already been conducted to correlate time series of subsets of these measured quantities. Part of the motivation for this is conceptual models for the chemical conversion of some constituents to others. Another

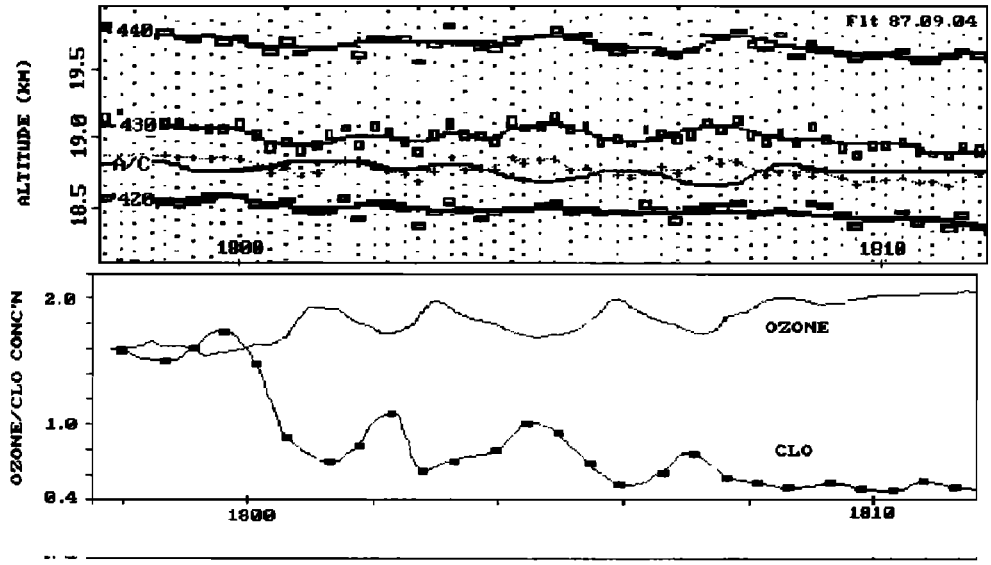

Fig. 8. (Top panel) Small oscillations in Θ surface altitude (120 m, peak-to-peak) and equally small out-of-phase oscillations in ER-2 flight level produce large oscillations (bottom panel) in such molecular species as chlorine monoxide and ozone. The dotted curve in the top panel corresponds to Θ = 426 K. The ozone and CLO variations are anticorrelated, showing a positive altitude gradient for ozone and a negative one for ClO. Apparently there is a layer of depleted ozone and high ClO below the ER-2 flight level.

motivating conceptual model envisions mixing of air masses, with long-lived tracers providing a "fingerprint" for air parcel origins.

Most flights involved flight segments along constant potential temperature surfaces. This strategy simplifies data interpretation by removing a potentially confounding variable from consideration. Air parcels that are on the same potential temperature surface constitute a family of potentially related parcels owing to the ease with which they can conceivably come into contact with each other. Air parcels at other potential temperature surfaces are insulated from contact with each other by an energy difference related to the difference in their potential temperatures.

Changes in the concentration of molecules during a latitude traverse will respond to penetrations of air that has undergone slightly different histories of chemical experience, such as a longer exposure to heterogeneous chemical reactions occurring on PSC particles. Other AAOE papers address the many interesting issues that can be dealt with using such time series correlations.

It is important to not be misled by subtle effects caused either by altitude oscillations of Θ surfaces or by unintended altitude excursions of ER-2 flight level. For example, in Figure 4 there are small variations of both Θ surfaces and flight level between 1800 and 1809 UT. The Θ surface variations are confined to altitudes above the Θ = 420 K surface. Figure 8 is an expanded version of the middle part of Figure 4.

In Figure 8 the Θ = 426 K surface has been indicated by a dotted trace. The combined effects of the 120-m out-of-phase oscillations of Θ surfaces and flight level lead to an effective oscillation of about 5 K across Θ surfaces. The bottom panel of Figure 8 shows the anticorrelated traces of ozone and ClO. They are in perfect phase with the altitude excursions. Ozone shows a positive gradient with Θ, while ClO shows a negative gradient. The amplitude of the ozone and ClO variations is 15% and 50%, respectively. Whereas it might have seemed reasonable to ascribe such large variations to horizontal structures when the ER-2 flight level is undergoing excursions of only 120 m, the evidence in Figure 8 suggests that a better interpretation is that the ER-2 was flying along the upper boundary of a layer of depleted ozone and high ClO, where small distortions of the Θ surface field can lead to dramatic changes in measured concentrations of molecular species.

Extreme layering of ozone depletions is known to occur, and perhaps a similar layering exists for ClO. The sense of the correlation is comprehensible and is consistent with ClO causing the destruction of ozone. The issues of time scales and maintaining steep vertical gradients are beyond the scope of this paper. Investigations of these correlations are described by *Anderson et al.* [this issue] *Murphy et al.* [this issue] and others. The purpose of this example is to convey caution to investigators who are endeavoring to interpret what may appear to be "level flight" correlated variations of chemical constituents and to point out that the potential temperature cross sections can be useful in identifying occasions when these altitude excursions could be a problem. (A complete set of Θ cross sections for the ER-2 AAOE flights is available from the author.)

7. Concluding Remarks

The Microwave Temperature Profiler was included in the ER-2 payload for the Airborne Antarctic Ozone Experiment for the purpose of detecting penetrations into and out of the polar vortex. This was to be done by noting changes in potential vorticity, which requires MTP measurements of air temperature lapse rate. As described by *Hartmann et al.* [this issue], potential vorticity has been successfully used to locate the polar vortex boundary for some of the flights. However, it appears that air temperature lapse rate does not change when penetrating the polar vortex (and therefore the horizontal wind gradient must be causing the potential vorticity changes).

The most significant result from the MTP observations is the unexpected discovery of mountain waves over the

Palmer Peninsula. During the 5-week period of observation, the average occurrence of mountain wave encounters when flying over the peninsula ranged from 64% at the south end to 30% in the north region. Wave amplitudes reached values as great as 1200 m (peak-to-peak). The mountain wave encounters always showed the presence of waves from the lowest altitude that could be measured to the highest. The ensemble of encounters shows an increase of amplitude with altitude that is in agreement with predictions from mountain wave theory.

The exact significance of the finding that mountain waves exist, and may even be common, over Antarctica is difficult to assess at this time. Speculations have been made (*A. Y. Hou and K. W. Ko*, personal communication, 1987; D. Cariolle, personal communication, 1989) concerning the possible role that mountain waves may play in creating and sustaining the ozone hole. It is expected that future papers will address this potentially important matter.

APPENDIX: RADIATIVE TRANSFER CONCEPTS USED IN INTERPRETING MTP DATA

The MTP is a passive microwave radiometer that measures thermal emission of oxygen molecules. The measured quantity is commonly referred to as "brightness temperature." Brightness temperature is directly related to the number of radio photons intercepted by an antenna per unit bandwidth per unit time. A perfectly absorbing/emitting target that fills the antenna beam will duplicate the number of intercepted photons, when it is brought to a physical temperature equal to the measured brightness temperature. This, indeed, is the definition for brightness temperature.

The atmosphere is a perfect absorbing material, provided that it is thick enough. When the atmosphere is thick, and when it is uniform in temperature, the measured brightness temperature will equal the physical temperature of the atmosphere. When the atmosphere is not thick enough, such as to absorb only 90% (for example) of radio photons incident upon it, the measured brightness temperature will be 90% of the atmosphere's physical temperature. This situation exists for use of the MTP instrument at flight levels of 70,000 feet (~21.3 km) and viewing directions of +60°. The corrections that are required are called "transparency corrections," and they can amount to as much as 30 K.

Considering the situation of a sufficiently thick atmosphere, which is not uniform in temperature throughout, the measured brightness temperature will be a weighted average of the physical temperature along the viewing direction. The following equation (the radiative transfer equation) describes how this "weighting" occurs:

$$TB = \int_{r=0}^{\infty} K\alpha(r)*(1 - e^{-\tau})*T(r)*dr \div \int_{r=0}^{\infty} K\alpha(r)*(1 - e^{-\tau})*dr \qquad (1)$$

where

$$\tau = \tau(r) = \int_{r'=0}^{r} K(r')*dr'$$

and where TB is brightness temperature (in Kelvins), r is range (in kilometers) along the viewing direction, $K\alpha(r)$ is an absorption coefficient (in nepers per kilometer) at range r produced by the propensity of oxygen molecules to interact with radio photons, $T(r)$ is oxygen molecule physical temperature (in Kelvins) at location r, and τ is optical depth (defined above).

The first two terms in the denominator in (1), taken together, define a "weighting function." It decreases exponentially from 1 (at $r = 0$) to 0 (at $r = \infty$), The weighting function is $1/e$ at a range that is commonly referred to as the "applicable range." This range is important in the class of remote sensing situations involving the above radiative transfer equation (1). Whenever a decreasing exponential weighting function is multiplied with a uniformly varying source function, the weighted average of this integral multiplication has a value equal to the source function value at the weighting function's $1/e$ location. For MTP, when the applicable range is 1 km, for example, and when the atmosphere's temperature varies linearly with range (that is, altitude), the measured TB will equal air temperature at the range of 1 km. This gives rise to the term "applicable altitude," defined to be the applicable range multiplied by the sine of the elevation angle. The applicable altitude is the altitude where the weighting function, plotted against altitude, is $1/e$.

For the case when the atmosphere is opaque and air temperature $T(h)$ varies linearly with altitude h, a simple conversion of "observables" to "retrievables" (air temperature at specified altitudes) is possible:

$$T(h) = TB(h')$$

where h' is equal to (applicable range) * (sine of elevation angle), and TB is the measured brightness temperature at the specified elevation angle. For this situation the task reduces to merely knowing the applicable range, which is approximately $1/K\alpha$, where $K\alpha$ is the oxygen absorption coefficient at flight level. $K\alpha$ is a function of air density and air temperature, but its dependence on these air properties is well known. (Actually, $K\alpha$ varies with altitude, so an additional effect must be modeled when the actual algorithm for retrieving air temperature from observables is designed. A description of considerations at this level of detail is beyond the scope of this paper, but they are available from the author.)

Difficulties arise when the source function $T(r)$ does not vary linearly with range, which occurs when air temperature $T(h)$ does not vary linearly with altitude h. There is no problem when the $T(h)$ inflection is at the aircraft altitude, however, for in this case, air temperature varies linearly with range for all elevation angles. The difficulty occurs only when there are temperature structures at altitudes displaced above or below flight level (but not when these structures are very far away from flight level).

Several procedures are available for recovering from this problem. A statistical retrieval technique can be employed, as is common when using either ground-based or satellite-borne temperature profilers [*Westwater*, 1972]. The Backus-Gilbert approach [*Backus and Gilbert*, 1967] is a deterministic procedure that gives results comparable to the statistical method.

Another inversion procedure has been developed for use with MTP data, which is a "mutational search and evaluation of parameter space." Air temperatures are set to TB at altitudes corresponding to h', as described earlier (this set of $T(h)$ is hereafter referred to as "parameters"), then a series

of parameter mutations/observable set calculations/rms comparisons are conducted. The parameter mutations are made on at least two parameters at a time, which enables a more complete search of parameter space to be conducted. For each hypothetical set of parameter values, a direct calculation is performed of all observed quantities (the 15 observables). In performing this calculation, explicit use is made of temperature and pressure dependencies of oxygen molecules. Transparency effects are also explicitly taken into account. In calculating a rms between the calculated observables and the measured observables, a weighting system is employed which penalizes "altitude temperature structure" at altitudes far from flight level. With an AT microcomputer (having a math coprocessor) an altitude temperature profile "solution" can be found in about 5 s. Since a flight may have fourteen hundred 14-s observation cycles, about 2 hours of additional data reduction time is required to apply this retrieval procedure to all data of a flight. Random checks have shown that very little additional structure (beyond what exists in the *TB* versus h' plot) is recovered from a typical profile. Hence this recovery procedure is used only in "special case" studies, which will be described in future papers.

Acknowledgments. The research described in this paper was carried out by the Jet Propulsion Laboratory, California Institute of Technology, under a contract with the National Aeronautics and Space Administration. Specific acknowledgment is owed to Richard Denning, Steve Guidero, and Gary Parks for designing and constructing the Microwave Temperature Profiler instrument. Richard Denning and Steve Guidero participated in the observations in Punta Arenas, Chile. Data were generously provided by Roland Chan, Jim Anderson, and Patti Hathaway for use in the work described in this paper.

REFERENCES

Anderson, J. G., W. H. Brune, and M. H. Proffitt, Ozone destruction by chlorine radicals within the Antarctic vortex: The spatial and temporal evolution of ClO-O_3 anticorrelation based in in situ ER-2 data, *J. Geophys. Res.*, this issue.

Backus, G. E., and J. F. Gilbert, Numerical applications of a formalism for geophysical inverse problems, *Geophys. J. R. Astron. Soc.*, *13*, 247, 1967.

Chan, K. R., S. G. Scott, T. P. Bui, S. W. Bowen, and J. Day, Temperature and horizontal wind measurements on the ER-2 aircraft during the 1987 Airborne Antarctic Ozone Experiment, *J. Geophys. Res.*, this issue.

Denning, R. F., S. L. Guidero, G. S. Parks, and B. L. Gary, Instrument description of the airborne Microwave Temperature Profiler, *J. Geophys. Res.*, in press, 1989.

Hartmann, D. L., K. R. Chan, B. L. Gary, M. R. Schoeberl, P. A. Newman, R. L. Martin, M. Loewenstein, J. R. Podolske, and S. E. Strahan, Potential vorticity and mixing in the south polar vortex during spring, *J. Geophys. Res.*, this issue.

Holton, J. R., *An Introduction to Dynamic Meteorology*, p. 159, Academic, San Diego, Calif., 1979.

McKenna, D. S., R. L. Jones, A. T. Buckland, J. Austin, A. F. Tuck, R. H. Winkler, and K. R. Chan, The southern hemisphere lower stratosphere during August and September 1987: Analyses based on the United Kingdom Meteorological Office global model, *J. Geophys. Res.*, in press, 1989.

Murphy, D. M., A. F. Tuck, K. K. Kelly, K. R. Chan, M. Loewenstein, J. R. Podolsee, M. H. Proffitt, and S. E. Strahan, Indicators of mixing and vertical motion from correlations between in situ measurements in the Airborne Antarctic Ozone Experiment, *J. Geophys. Res.*, this issue.

Rosenkranz, P. W., Shape of the 5-mm oxygen band in the atmosphere, *IEEE Trans. Antennas Propag.*, *AP-23*, 498–506, 1975.

Westwater, E. R., Ground-based determination of low-altitude temperature profiles by microwaves, *Mon. Weather Rev.*, *100*, 15–28, 1972.

B. L. Gary, MS T-1182, Jet Propulsion Laboratory, 4800 Oak Grove Drive, Pasadena, CA 91109.

(Received May 2, 1988;
revised November 15, 1988;
accepted November 15, 1988.)